

A Low-Profile Broadband Dual-Polarized Antenna With Coupled Feed Structure and AMC for 5G Base Station Application

Hailong Zeng and Yejun He*

State Key Laboratory of Radio Frequency Heterogeneous Integration
Sino-British Antennas and Propagation Joint Laboratory, Ministry of Science and Technology of China
Guangdong Engineering Research Center of Base Station Antennas and Propagation
Shenzhen Key Laboratory of Antennas and Propagation
College of Electronics and Information Engineering, Shenzhen University, 518000, China
Email: 2310434078@email.szu.edu.cn, heyejun@126.com*

Abstract—In this article, a low-profile broadband dual-polarized antenna with a bilateral coupled feed and artificial magnetic conductor (AMC) is proposed. The antenna is composed of a radiating patch at the top, parasitic strips around it, a coupling feed structure under the radiating patch, a balun, an AMC structure and a slotted reflector at the bottom. The operating frequency band of the antenna is 0.69~0.96 GHz, and the overall size is small with low profile characteristics. It is 260 mm × 260 mm × 34.5 mm (approximately $0.718\lambda_0 \times 0.718\lambda_0 \times 0.096\lambda_0$), S_{11} and S_{22} are below -10 dB in the operating band, and the isolation between the two ports is lower than -24 dB. At the same time, it has a stable realization gain (8.16 ± 1.01 dBi) and maintains excellent cross-polarization discrimination (XPD). Finally, the antenna's front-to-back ratio (FTBR) is higher than 22 dB, which has low backward radiation characteristics. The half-power beamwidth (HPBW) in the XOZ plane is ($67.34^\circ \pm 6.13^\circ$), which meets the performance requirements for 5G base station antenna covering low frequency band.

I. INTRODUCTION

With the rapid advancement of communication systems, a vast number of dual-polarized base station antennas operating at different frequency bands have been extensively researched. Traditional base station antennas generally use a perfect electric conductor (PEC) as the reflector element. In antenna engineering, maintaining a distance of approximately $0.25\lambda_0$ from the reflector is a common practice to achieve optimal radiation performance [1]-[3]. Therefore, the implementation of a low-profile base station antenna not only leads to substantial cost savings in base station deployment but also enhances the antenna's ability to withstand various risks. The research of broadband dual-polarized low-profile base station antennas is of great importance in modern base station development.

Over the past few years, many researchers have focused on studying low-profile antennas and made significant academic progress. In reference [4], the antenna achieves a low-profile height of $0.12\lambda_0$ by incorporating a frequency-selective surface (FSS) between the radiators operating in the frequency range of 0.69~0.96 GHz. In [5], a low-profile dual-polarized dielectric resonator antenna was proposed. The antenna changes the electric-field distribution by slotting the dielectric resonator surface to improve the gain within the operating bandwidth. The antenna profile was as low as

$0.09\lambda_0$. [6] presents a low-profile dual-polarized base station antenna with an AMC reflector instead of a traditional metal reflector, achieving an impedance bandwidth from 1.69 GHz to 2.71 GHz. The overall antenna size is 150 mm × 150 mm × 18.8 mm (approximately $1.1\lambda_0 \times 1.1\lambda_0 \times 0.138\lambda_0$). It is worth noting that the process of reducing antenna height faces two major challenges: impedance mismatching and radiation pattern variation [7], with the former having a greater impact [8]. Therefore, the key concern after reducing antenna height is ensuring proper impedance matching.

This paper proposes a low-profile dual-polarized dipole antenna with a bilateral coupled feed structure, and AMC structure is used to replace the traditional reflector, featuring a stable radiation pattern tailored for base station applications. Different from the direct feeding and single-side coupled feeding of traditional base station antennas, the feeding method of the crossed-dipoles radiator is not in direct contact with the balun feeding structure, but in direct contact with the coupled feed structure on the back of the substrate. Such a feeding method brings about the effect of low profile. The proposed antenna's height is restricted to a mere $0.096\lambda_0$, a notable reduction compared to the conventional $0.25\lambda_0$. Simulation results confirm that the proposed antenna is a reliable candidate for base station applications in antenna engineering.

II. ANTENNA DESIGN

The configuration of the proposed antenna is illustrated in Fig. 1. It is mainly composed of the following parts: the radiation patch printed on the top of the dielectric substrate, with the parasitic strip placed around it, and the coupling feed structure is located on the lower surface of the dielectric substrate; two feeding baluns are placed orthogonally to connect the coupling feed structure and the reflector plate; the AMC structure consists of an 8×8 metal patch printed on the front side of the substrate and placed horizontally between the reflector and the planar dipole; the bottom is a special-shaped reflector.

The materials of the radiating components, such as the radiation patch, parasitic strip, and reflector plate, are alu-

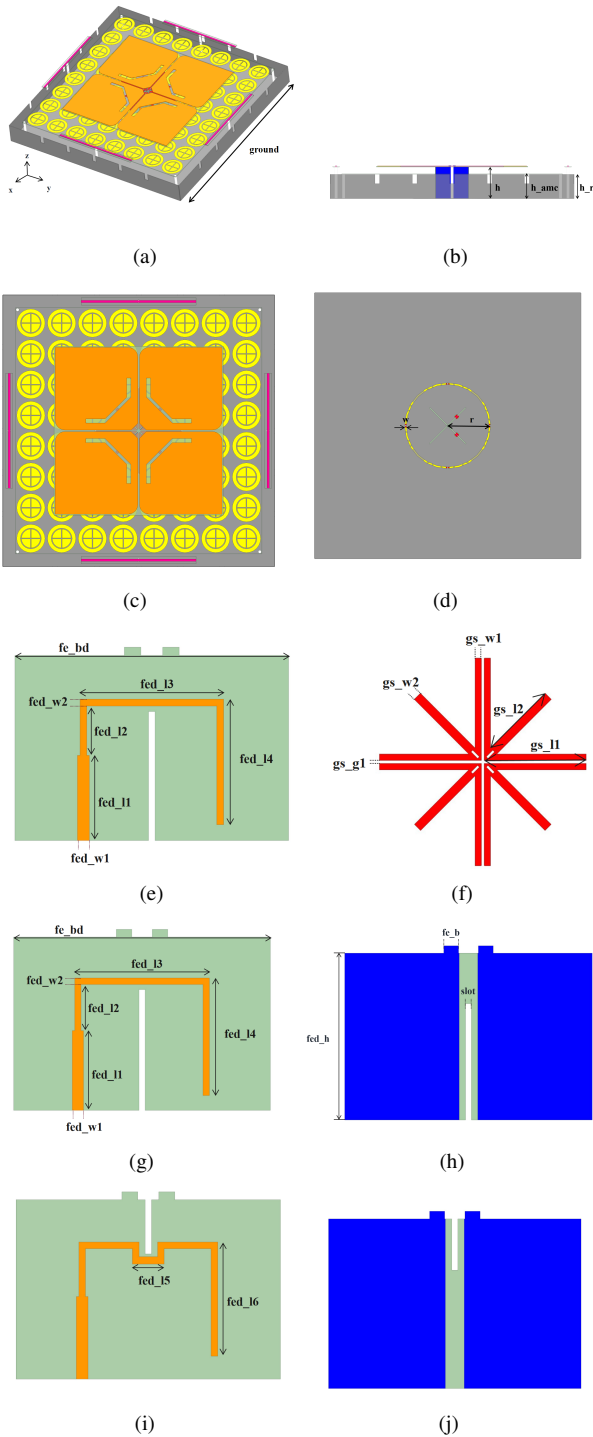


Fig. 1. Configuration of the antenna. (a) 3D view; (b) Side view; (c) Top view; (d) Reflector bottom and ring slot; (e) Main radiator; (f) Coupling feed structure; (g) Front of balun 1; (h) Back of balun 1; (i) Front of balun 2; (j) Back of balun 2.

minum plates with a thickness of 0.5 mm. The coupling feed structure and the balloon structure consist of a 0.035-mm-thick copper layer, which is printed on the dielectric substrate. The dielectric substrate used for the entire antenna is FR4, with the following properties: a relative dielectric constant of 4.4,

a loss tangent of 0.02, and a single-layer thickness of 0.762 mm.

The main radiator of the proposed antenna adopts a four-patch configuration, which forms a pair of dipoles placed orthogonally, and the dual polarization can be achieved by excitation of them respectively. Each patch is chamfered to reduce mutual coupling, and a U-shaped slot is arranged in the center of the patch to prolong the current path. After that, four parasitic strips are placed at the center of the perimeter, which can be used to expand the impedance bandwidth. At the same time, when the main radiator is excited, the current induced on the parasitic strips helps to improve the XPD of the antenna.

As shown in Fig. 2, the periodic structure simulation and reflection characteristics of the AMC unit are presented. A traditional metal reflector causes a 180° phase shift, requiring placement below the antenna at $0.25\lambda_0$. In contrast, an AMC reflector approximates a perfect magnetic conductor (PMC) with zero-phase reflection, allowing it to be positioned closer to the antenna for improved radiation efficiency. The reflection phase of the AMC ranges from -90° to $+90^\circ$ within the operating bandwidth. The bandwidth of traditional circular AMC is relatively narrow. To achieve broadband reflection, an air layer is introduced into the structure, effectively increasing the thickness of the dielectric substrate. Additionally, slots are incorporated to introduce capacitive loading, thereby adjusting the bandwidth and achieving broadband reflection characteristics.

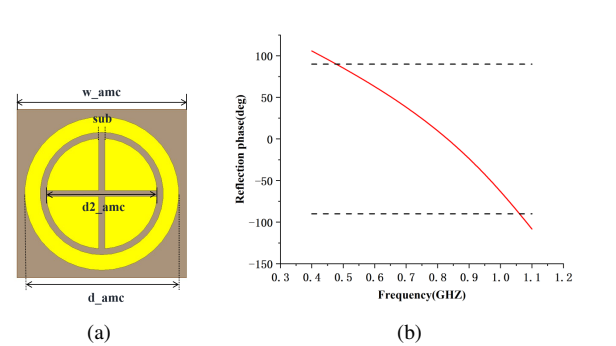


Fig. 2. Configuration of the antenna. (a) AMC structure; (b) Reflection phase of the AMC structure.

The balun consists of a substrate, a microstrip line printed on the front side, and a slot line printed on the back side. To ensure the balun's performance remains as consistent as possible, a section of the front microstrip line is shifted downward to enhance isolation.

To increase the front-to-back ratio of the antenna, an irregular-shaped reflector is used. Periodic slits are made at the edges of the reflector to reduce the induced current on the edges of the reflector. As illustrated in Fig. 3, the strong backward radiation is caused by the diffraction field [9] at the edges of the narrow reflector. To reduce backward radiation and further improve the antenna's front-to-back ratio, circular-shaped slots are etched on the reflector. The slots generate

transmission fields in the back lobe region. By adjusting the size and spacing of the slots, the amplitude and phase of the transmission fields can be controlled. The transmission fields are used to cancel the backward fields generated by the baffles, thereby reducing the backward radiation. The dimensions of the proposed antenna are listed in Table I. The antenna was simulated and optimized using HFSS software.

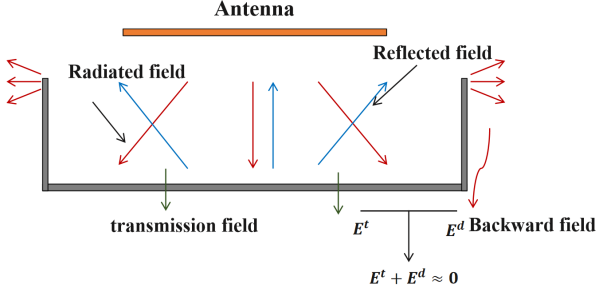


Fig. 3. Working principle for the circular-shaped slots on the reflector.

TABLE I
THE OPTIMIZED PARAMETERS OF THE PROPOSED ANTENNA(UNIT: MM)

Parameter	<i>ground</i>	<i>h</i>	<i>h_r</i>	<i>h_{amc}</i>
Value	260	34.5	26	26
Parameter	<i>r</i>	<i>w</i>	<i>gs_l</i>	<i>gs_g</i>
Value	42	1.5	159.7	1.7
Parameter	<i>gs_a</i>	<i>v_w</i>	<i>l1</i>	<i>l3</i>
Value	9	4	35	13
Parameter	<i>gs_{w1}</i>	<i>gs_{w2}</i>	<i>gs_{l1}</i>	<i>gs_{l2}</i>
Value	2	2.8	41	25
Parameter	<i>gs_{g1}</i>	<i>fe_{bd}</i>	<i>fed_{l1}</i>	<i>fed_{l2}</i>
Value	1	50	15	9
Parameter	<i>fed_{l3}</i>	<i>fed_{l4}</i>	<i>fed_{l5}</i>	<i>fed_{l6}</i>
Value	26.25	21	6	20.2
Parameter	<i>fed_{w1}</i>	<i>fed_{w2}</i>	<i>sub</i>	<i>w_{amc}</i>
Value	2.2	1.25	1	29.5
Parameter	<i>d_{amc}</i>	<i>d2_{amc}</i>	<i>fe_b</i>	
Value	27	18	3	

III. SIMULATION RESULTS

Fig. 4 illustrates the impact of the coupling feeding on the $|S_{11}|$ characteristics of the antenna, including cases with and without coupling feeding. The use of coupled feed structures introduces new resonance points, which greatly expands the bandwidth.

The simulation results of antenna scattering parameters and gain are shown in Fig. 5(a). It can be seen that the impedance bandwidth of the proposed antenna when port 1 ($+45^\circ$ polarization) and port 2 (-45° polarization) are excited includes $0.69\sim 0.98$ GHz, and the S_{11} and S_{22} are less than -10 dB in the frequency band. At the same time, the S_{12} is below -24 dB across the operating band, achieving a peak isolation of -36 dB. This outstanding isolation performance effectively

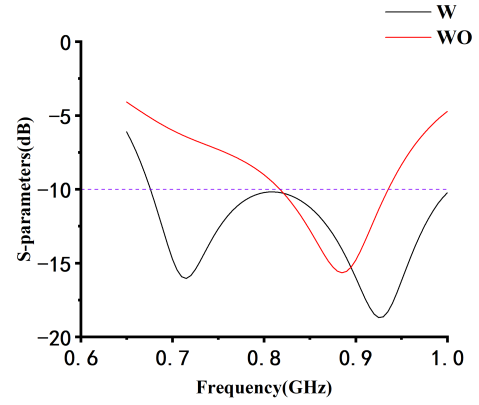


Fig. 4. The influence of coupling feeding on antenna impedance matching.

suppresses mutual coupling between antenna elements. As illustrated in Fig. 5(b), the simulated gain is 8.16 ± 1.01 dBi, and the HPBW consistently maintains stability at $67.34^\circ\pm 6.13^\circ$ in Fig. 5(c), within the designated operating band. Finally, Fig. 5(d) shows the total efficiency of the antenna in the frequency band, with a minimum efficiency of 93%.

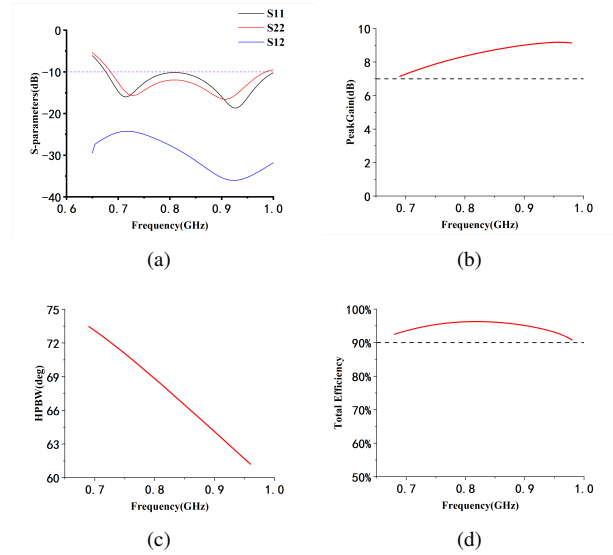


Fig. 5. Simulation results of the proposed antenna: (a) Simulation S-parameters; (b) Realized gains of the proposed antenna under the excitation of port 1; (c) HPBW of the proposed antenna under the excitation of port 1; (d) Simulated total efficiency of the proposed antenna.

Fig. 6 shows the simulated front-to-back ratio of the proposed antenna by using different reflectors. It is clear that the front-to-back ratio of the proposed antenna is improved by 5 dBi approximately, improved from $15.5\text{-}20.1$ dBi to $20.4\text{-}23.2$ dBi.

Fig. 7 shows the cross-polarization characteristics of 0.69 GHz, 0.78 GHz, 0.87 GHz, and 0.96 GHz on the XOZ plane of the antenna when the $\pm 45^\circ$ polarization excitation. the XPD of the proposed antenna surpasses 24 dB at 0° and more than 11.4 dB at $\pm 60^\circ$, which has excellent cross-polarization discrimination. At the same time, the radiation pattern of the

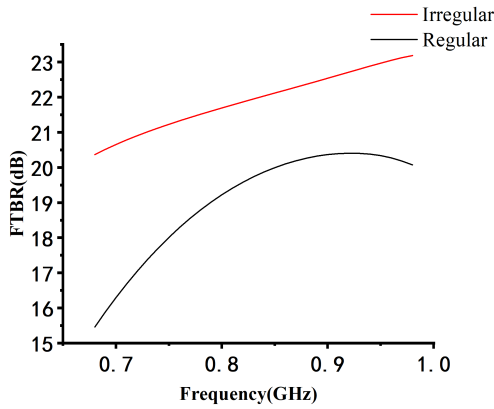


Fig. 6. The influence of different reflectors on the front-to-back ratio of the antenna.

antenna remains stable in the whole frequency band, and is only slightly narrowed due to the change of radiation aperture caused by the change of frequency.

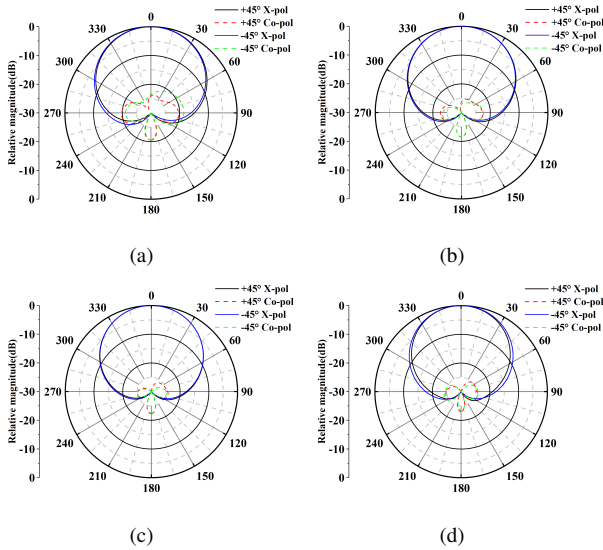


Fig. 7. Simulated radiation patterns of the proposed antenna. (XOZ plane):(a) 0.69 GHz; (b) 0.78 GHz; (c) 0.87 GHz; (d) 0.96 GHz.

IV. CONCLUSION

In this paper, a low-profile, broadband, dual-polarization antenna with an AMC and an electromagnetic bilateral coupling feeding structure is proposed for the 0.69~0.96 GHz frequency band. The introduction of AMC and coupling feed structures has effectively reduced the antenna profile while addressing the impedance mismatch problem caused by the reduced profile. In addition, the inclusion of parasitic branches around the antenna significantly improves cross-polarization discrimination. Finally, a reflective plate is added to the bottom of the antenna. To enhance the front-to-back ratio, a circular ring-shaped gap is introduced beneath the reflector plate, and periodic slots are incorporated along the metal edge, which effectively improves the front-to-back ratio and reduces

backward radiation. The performance of the proposed antenna meets the requirements of practical base station antenna applications.

ACKNOWLEDGEMENT

This work is supported in part by the National Key Research and Development Program of China under Grant 2023YFE0107900, the National Natural Science Foundation of China (NSFC) under Grant 62071306, and the Shenzhen Science and Technology Program under Grants JSG-G20210802154203011, JCYJ20241202124219023, and JSG-G20210420091805014.

REFERENCES

- [1] H. Huang, Y. Liu and S. Gong, "A Broadband Dual-Polarized Base Station Antenna With Sturdy Construction," *IEEE Antennas and Wireless Propagation Letters*, vol. 16, pp. 665-668, 2017.
- [2] S. Yang, L. Liang, W. Wang, Z. Fang and Y. Zheng, "Wideband Gain Enhancement of an AMC Cavity-Backed Dual-Polarized Antenna," *IEEE Transactions on Vehicular Technology*, vol. 70, no. 12, pp. 12703-12712, Dec. 2021.
- [3] L. H. Ye, D. G. Ye, Z. Chen and J. F. Li, "Ultra-Wideband Dual-Polarized Base-Station Antenna With Stable Radiation Pattern," *IEEE Transactions on Antennas and Propagation*, vol. 71, no. 2, pp. 1919-1924, Feb. 2023.
- [4] Y. Zhu, Y. Chen and S. Yang, "Decoupling and Low-Profile Design of Dual-Band Dual-Polarized Base Station Antennas Using Frequency-Selective Surface," *IEEE Transactions on Antennas and Propagation*, vol. 67, no. 8, pp. 5272-5281, Aug. 2019.
- [5] Q. Wu, H. Li, S. -W. Wong, Y. -C. Lin and Y. He, "A Low-Profile Dual-Polarized Dielectric Resonator Antenna for 2G/3G/4G Base Station Applications With Gain Enhancement," in *Proc. 2024 IEEE International Workshop on Radio Frequency and Antenna Technologies (iWRFAT)*, Shenzhen, China, 2024, pp. 486-488.
- [6] Z. Lu, Y. Chen, X. Chen and R. Ma, "A low profile dual polarized antenna with AMC reflector for base stations," in *Proc. 2020 International Conference on Microwave and Millimeter Wave Technology (ICMMT)*, Shanghai, China, 2020, pp. 1-3.
- [7] M. Li, M. Y. Jamal, C. Zhou, L. Jiang and L. K. Yeung, "A Novel Dipole Configuration With Improved Out-of-Band Rejection and its Applications in Low-Profile Dual-Band Dual-Polarized Stacked Antenna Arrays," *IEEE Transactions on Antennas and Propagation*, vol. 69, no. 6, pp. 3517-3522, June 2021.
- [8] C. Zhou, J. Sun, W. -W. Yang, M. Li and H. Wong, "A Wideband Low-Profile Dual-Polarized Hybrid Antenna Using Two Different Modes," *IEEE Antennas and Wireless Propagation Letters*, vol. 22, no. 1, pp. 114-118, Jan. 2023.
- [9] X. Deng, Y. Chen and S. Yang, "Improving Front-to-Back Ratio of Base Station Antenna Array With a Modified Reflector," in *Proc. 2023 IEEE MTT-S International Wireless Symposium (IWS)*, Qingdao, China, 2023, pp. 1-3.